Journal of Water Process Engineering 49 (2022) 103032

Contents lists available at ScienceDirect

Journal of Water Process Engineering

journal homepage: www.elsevier.com/locate/jwpe

Effective separation of petroleum oil-water mixtures via flexible and re-usable hydrophobic soot-coated melamine sponge

Meruyert Nazhipkyzy [a,b,*], Dana Assylkhanova [a,b], Nurgain Araylim [a,b], Aigerim Seitkazinova [a], Gamzenur Özsin [c,d], Esin Apaydın Varol [e]

[a] Al-Farabi Kazakh National University, Faculty of Chemistry and Chemical Technology, Almaty 050000, Kazakhstan
[b] Institute of Combustion Problems, Laboratory of Synthesis Carbon Nanomaterials in Flame, Almaty 050000, Kazakhstan
[c] Bilecik Şeyh Edebali University, Faculty of Engineering, Dept. of Chemical Engineering, Bilecik, Turkey
[d] Imperial College London, Faculty of Engineering, Dept. of Chemical Engineering, SW7 2BU London, UK
[e] Eskişehir Technical University, Faculty of Engineering, Department of Chemical Engineering, 26555 Eskişehir, Turkey

ARTICLE INFO

Keywords:
Soot
Hydrophobicity
Hydrophobic sponge
Adsorption
Oil-water separation

ABSTRACT

Superhydrophobic materials like carbon-coated sponges have been attracting attention due to their wide applicability in several industries. One of the main applications of such materials is the efficient removal of various water pollutants such as oil by adsorption. Herein, a flexible, porous, and hydrophilic melamine sponge was coated by superhydrophobic soot that was produced by incomplete combustion of the propane-butane mixture. Characterization of the soot and the sponge was performed via several methods such as spectroscopy, microscopy, and thermogravimetry. The product was tested in the petroleum oil removal process. The superhydrophobic sponge repelled water well and at the same time perfectly sorbed oil products. The wetting edge angle of soot coated sponge was found between 145 and 150°. The sponge showed an excellent adsorption capacity of 24 g oil/g for the selective separation of oil from water. The entrapped oil was released simply by squeezing the sponge for cyclic use and about 95.5 wt% of the oil was adsorbed and the soot-coated sponge still maintained this capacity after 19 cycles. Hence, this novel soot-coated hydrophobic sponge is considered a promising candidate for oil-polluted water treatment.

1. Introduction

Water on earth is one of the most abundant natural resources, but only about 1 % of that resource is available for human consumption. It is known that over 1.1 billion people lack a supply of adequate high-quality water, due to the growing population, and a variety of climatic and environmental effects [1–3]. The majority of the pollutants in drinking water are arising from industrial, agricultural, and mining activities that lead to an increase in toxic materials contamination [4]. In addition to these inorganic contaminants, organic pollutants from volatile organic compounds, synthetic organic compounds, oil spills, and waste disposal are the main reasons for water pollution which have reprotoxic, carcinogenic, and mutagenic effects [5]. Especially, spillage of petroleum hydrocarbons during exploration, production, transportation, storage, and utilization of oil causes serious environmental pollution [6,7]. Oil spills are known among the most extensive and environmentally damaging pollution problems [8]. When petroleum oil is emulsified in water, problems generate ecological changes and negative impacts on aquatic life such as threatening the lives of fauna and the food chain due to the destruction of arable farmlands and fishing areas. The greatest concern of such spills is the long-term effects of both acute and chronic contaminations that can cause diseases for decades or more [9]. Therefore, significant research has been devoted to remedial technologies for oil-water separation across the globe [10].

Currently, several treatment processes for oil/water separation have been investigated such as chemical methods (dispersion, solidification), in-situ burning, bioremediation, and mechanical recovery [11]. However, most of these methods are considered non-viable due to their cost, creation of secondary pollution, having low selectivity and efficiency towards petroleum contaminants [3,11]. The oil/water separation process by physical sorption has always been the subject of active research since it is one of the most effective and inexpensive methods that offer good recyclability of the adsorbents. Various sorbent materials are aimed at removing and remediating oil spills which may be in the form

* Corresponding author at: Al-Farabi Kazakh National University, Faculty of Chemistry and Chemical Technology, Almaty 050000, Kazakhstan.
E-mail address: meruert82@mail.ru (M. Nazhipkyzy).

https://doi.org/10.1016/j.jwpe.2022.103032
Received 9 April 2022; Received in revised form 19 July 2022; Accepted 27 July 2022
Available online 1 August 2022

of powders, foams, and fabrics [12]. But some challenges remain in the adsorption technology such as improving expertise in developing selective sorbents and reducing the manufacturing cost using low-cost precursors. The important point is the production of adsorbents with superior capacity and selectivity which means they are capable of primary removal of petroleum oil rather than water. Moreover, reusability and regeneration characteristics are the other factors that should be considered in the selection of sorbent materials. There has been an increasing amount of research on the fabrication of oil-adsorbing materials, aiming at the separation of oils from water [11]. At this point, tailoring materials with specific wettability using the basics of chemistry and nanotechnology for oil-water separation is essential to developing feasible water remediation processes [13].

In the literature some natural sorbents have shown promising results, making them potential candidates for oil adsorption from the aqueous medium. On the other hand, synthetic sorbents, such as waste material or a side product of industrial processing, have promising results [14]. Especially, carbon-based adsorbents have been considered to be the best candidates in the field of oil spill cleanup as they possess high surface area, low density, good chemical stability, and large pore volume. Some carbon materials including carbon aerogels, graphene or carbon nanotube coated sponges, graphene foams or sponges, activated carbon, porous carbon nanoparticles, and activated carbon fibers have already been successfully applied for adsorption-based separation and purification processes [15–17]. This is due to the existence of several physiochemical mechanisms/forces, such as Van der Waals, hydrogen bonding, dipole-dipole interactions, ion exchange, covalent bonding, and cation-bridging and water-bridging, during the adsorption on the carbons [18]. Furthermore, carbons with different morphology and functionality may be obtained by adjusting precursor, production method, and conditions together with post-treatments such as modification [19].

In this study, special attention was paid to the use of carbonaceous soot to prepare a superhydrophobic material for the oil-spill clean-up process. Soot can be simply defined as a carbon material that is generated from the incomplete combustion of hydrocarbons. It is well-known that soot has remarkable advantages in the cost-effectiveness and production scalability over other carbon materials like graphene, carbon nanotube, and activated carbons in their synthesis. Moreover, when soot is examined in sorption processes it shows good adsorption capacity towards several pollutants and has good recyclability due to its chemical stability [20,21]. In addition, it can be easily modified to have magnetic properties to achieve better separation characteristics [22–24]. A broad literature survey pointed out the applicability of the soot in such kinds of adsorption studies but to our knowledge, there are no studies that formally test the ability of sponges in cyclic petroleum oil adsorption which incorporates soot of propane-butane combustion flame into the melamine matrix. The oil-removal application of straightforward and easily producible soot-coated sponges, with a high capacity and reusability, is the essential feature of this study. Within the scope of this study, superhydrophobic soot was produced from propane-butane mixture to obtain a hydrophobic sponge by coating technique. Due to having high-strength, low cost, and lightweight features together with good chemical and thermal resistance, the melamine sponge was selected as a template. Highly porous melamine sponge (over 99 % porosity), commercially known as magic eraser, and its composites can be utilized as adsorbents for several water cleaning purposes. The hydrophilic character of melamine sponge is its drawback for water applications and therefore the properties of melamine sponge are modified to achieve more suitable materials. Among the several modification techniques of melamine sponge, coating its surface with a carbon material via a simple dip and dry method seems to be a promising one for oil-water separation processes. Typically, graphene oxide or reduced graphene oxide nanoparticles are preferred as the coating material to enhance the mechanical strength of the pristine sponge and to obtain a hydrophobic structure [25–27]. The novelty of this study is that it is the first to explicitly examine the oil sorption behavior of soot-coated melamine sponge by employing cyclic adsorption tests which are combined with propane/butane-based soot production. Overall, a method to critically understand the contribution of soot-deposition to the sponge for water treatment, which can guide rationally fabricating high-capacity and easily regenerative adsorbents in the future, is provided.

2. Materials and methods

2.1. Reagents and materials

For the synthesis of soot, propane, and butane gas (85:15 vol./vol.) mixture (manufacturer “Ushkyn”, Universal gas all-season) was used. Melamine sponge was purchased from York company-Republic of Belarus. All the reagents and chemicals used in the synthesis are of analytical grade. For the adsorption of oil, petroleum from the Zhanaozen region of Kazakhstan is used without any pretreatment.

2.2. Synthesis of the soot

The synthesis of superhydrophobic soot was carried out in the flame of a propane-butane mixture by applying an electric field. Fig. 1 shows a diagram of the synthesis apparatus. A special generator drives a steel drum with a diameter of 12.5 cm, and a length of 13.5 cm. The principle of operation of the installation is based on the deposition of soot particles from the flame on the surface of a rotating drum (cylinder) and its automatic collection into a soot collector using a built-in scraper. The structure and properties of soot particles depend on the temperature in the flame volume. Since the formation of a soot particle does not occur instantly, but through a sequence of reactions, its structure and properties will also depend on the collection of soot at a certain level of its growth. The distance between the drum and the burner (normally 2.0 cm) is an important operating condition and increasing the distance over 3.0 cm leads to an increase in the amount of forming soot. The optimal mode of formation of soot having a superhydrophobic property is obtained at a collection distance of 2.0 cm with a contact angle of $>150^{\circ}$.

In this work, the soot was synthesized in the 1 kV current field under the action of incomplete combustion of propane-butane mixture under optimal conditions. The flow rate of the supplied gas was between 425 and 500 $cm^3 \cdot min^{-1}$. The rate of soot synthesis was equal to 0.005 $g \cdot min^{-1}$.

2.3. Characterization of the soot

The soot sample prepared as described above was characterized in terms of thermal stability, surface characteristics, morphology, and other physicochemical properties.

Thermogravimetric analysis (TGA) was implemented on an analyzer (Setaram Labsys Evo) with a heating rate of 20 $^{\circ}C \cdot min^{-1}$ under nitrogen or air atmospheres with a flow rate of 20 $mL \cdot min^{-1}$ to observe the stability of the soot sample against elevated temperatures. 10 ± 0.3 mg of sample was placed in a 100 μL alumina crucible and placed in TGA. Prior to the heating step, the furnace chamber was kept at 25 °C for 35 min under N_2 atmosphere to reach steady conditions.

The real density of the soot sample was measured using a Quantachrome-UltraFoam 1200e Helium pycnometer. Approximately 2 cm^3 of the sample was placed in the measurement cell and 5 runs were carried out to calculate the average density and standard deviation. The particle size distribution of soot was measured by a particle size analyzer (Dynamic Light Scattering, DLS, Malvern Nano-Sizer ZS), with ethanol as a dispersing agent. To achieve homogeneity, a sufficient amount of carbon sample was well dispersed in ethanol using an ultrasonic bath for 5 min.

The surface morphology of the samples was investigated with a scanning electron microscope (SEM) (Carl Zeiss Supra 40VP). Before the SEM analysis, samples were coated with Au and Pd using a sputter coater

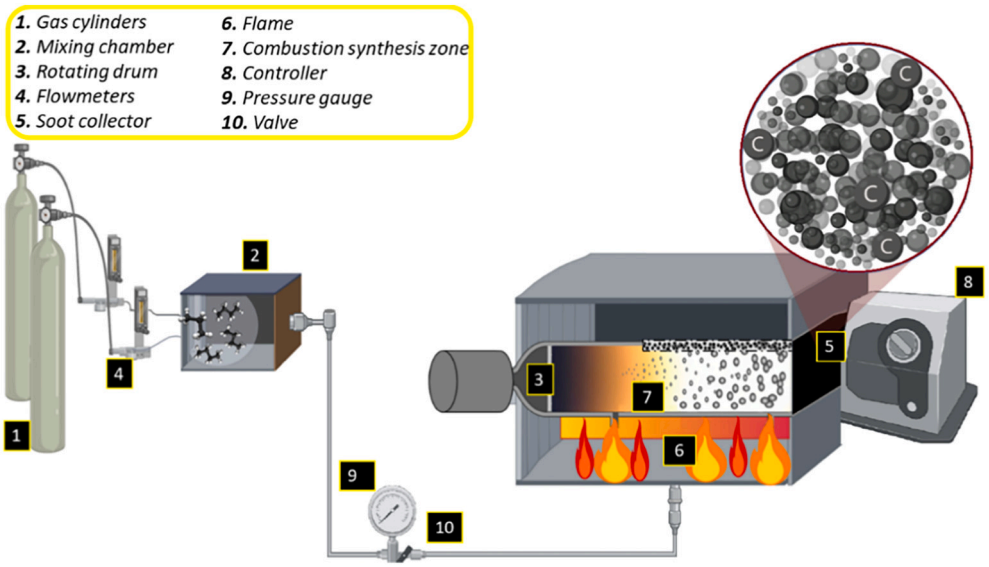

Fig. 1. Schematic representation of experimental set-up used in the soot production.

to minimize sample charging. Secondary electron micrographs were taken at several magnifications.

The pore characteristics and specific surface area (SSA) were determined by multi-point N_2 adsorption/desorption isotherms at −196 °C using Quantachrome Autosorb. Prior to N_2 adsorption, soot was degassed at 150 °C for at least 12 h. Using Brunauer–Emmett–Teller (BET) equation, SSA was determined.

FT-IR spectroscopy was carried out in the wavenumber range of 4000–400 cm^{-1} using a spectrometer (Thermo scientific Nicolet is10). The samples were well mixed with KBr at a weight ratio of 1:99 and the mixture was pressed into pellets under 8–10 tons of pressure for 10 s. The scan time and spectral resolution were 32 and 4 cm^{-1}, respectively.

The Raman characterization of carbon-based samples was performed on a Raman spectrometer (NTEGRA Spectra. Raman, $\lambda = 473$ nm, the area signals with a diameter of 80 nm). The X-ray diffractogram (XRD) of soot was recorded using an X-ray diffractometer (Miniflex 600 W, RIGAKU) with Cu Kα radiation (1.5436 Å, 40 kV, 15 mA). The diffraction patterns were recorded in the 2θ range of 10–90° with an increment of $2^{\circ}\cdot min^{-1}$. The graphitization degree of the sample was calculated according to the following equation [28–30]:

$$Graphitization\ degree\ (\%) = \frac{0.3440 - d_{002}}{0.3440 - 0.3354} * 100 \quad (1)$$

where 0.3440 nm and 0.3354 nm are the interlayer spacing of fully non-graphite crystals and the ideal graphite crystals, respectively. d_{002} is the interlaying spacing and can be calculated by Bragg's Law [28,29]:

$$d_{002} = \frac{n\lambda}{2Sin(\theta)} \quad (2)$$

where n is the order of the diffraction ($n = 1$), λ is the emission wavelength (0.15406 nm), and θ is the peak position in Radians for (002) peak.

2.4. Preparation and characterization of superhydrophobic sponge

25 mg of the soot was dispersed in a 20 mL solution of dichloroethane, after which a 60-minute ultrasound treatment was performed. Then the melamine sponge, which was cleaned with acetone and dried in an oven at 80 °C, was immersed in the soot dispersion. The sponge covered with soot was dried again in the oven at a temperature of 80 °C for 2 h.

After coating the melamine sponge with superhydrophobic soot, its water flotation behavior was tested and compared with the as-received melamine sponge. As shown in Fig. 2, the coated melamine sponge with superhydrophobic soot seemed to float easily on the surface of the water, which can be an indication of its applicability for the liquid-phase selective adsorption processes.

The wetting contact angle was measured using a drop shape analyzer DSA25 KRÜSS GmbH Kruss device. The accuracy of the device is 0.1°. The experiments were carried out at 25 °C, under 931 MPa, and at a humidity of 60–80 %. Distilled water was used for all the experiments. A 2.00 μL drop of water was dosed on the sample. After 5 s of stabilization, the wetting angle of the sample surface was measured.

The effect of acid and alkali conditions on the mechanical characteristics of the soot-coated sponge was studied in detail. The product was placed into 1 M HCl and NaOH solutions for 3 h of exposure. Cyclic compressing, bending, and twisting behaviors were tested together with tensile strength measurements to investigate the acid and alkali resistance of the soot-coated sponges. The tensile strength of the sponges at ambient temperature was measured using an electronic tensile machine (Jinan Hensgrand WDW-50E) for the samples prepared in the same dimensions (2 cm × 2 cm × 1 cm). The drawing speed was 5 $mm\cdot min^{-1}$ and the clamping distance was 200 mm.

2.5. Oil-water separation

For the oil-water separation experiments, petroleum from the Zhanaozen deposit of the West Kazakhstan region was used. To study the adsorption properties, the oil-water mixture was prepared as follows: 35 mL of distilled water was poured into a petri dish and ~3.0 mL of petroleum oil was added. A sponge with dimensions of 2 cm × 2 cm × 1 cm was placed on the surface of the water-oil mixture and the sponge was allowed to fully adsorb the oil (Fig. 3). To confirm the hydrophobic characteristic of the coated sponge for the adsorption of oil in the aqueous phase, the adsorption capacity was tested in batch experiments. The time required for the sorption was noted to calculate the adsorption rate. Desorption was carried out by simple compression of the sponge and then to completely remove the oil sponge was washed in benzene. The adsorption-desorption experiments were repeated until reaching a point where the oil sorption capacity decreased. All adsorption-desorption experiments were performed at least three times to ensure repeatability. The weight of the superhydrophobic sponge was measured before and after sorption experiments to calculate the sorption capacity. The equation used for the calculation of the oil sorption capacity is:

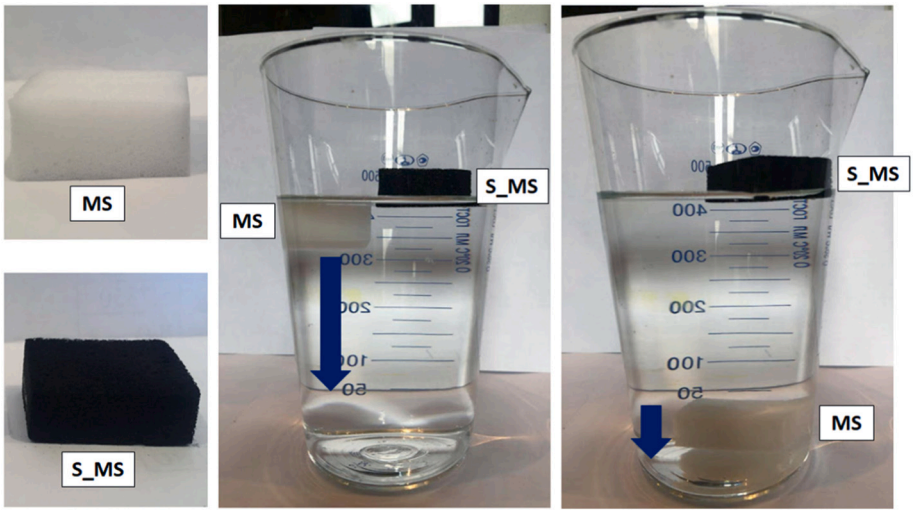

Fig. 2. The hydrophobicity of raw (MS) and soot-coated melamine sponge (S_MS) (MS is submerged in water and S_MS is floating).

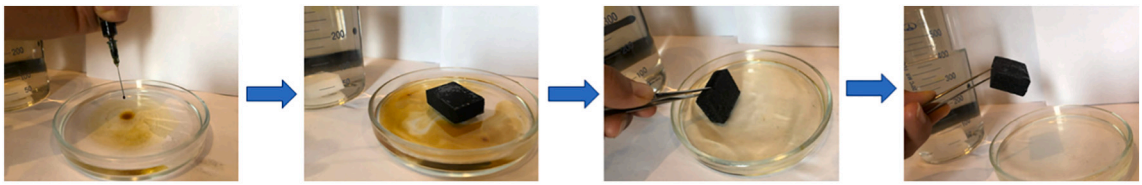

Fig. 3. Visualization of the steps in the oil adsorption testing of hydrophobic soot-coated sponge.

$$Oil\ sorption\ capacity = \frac{weight\ of\ adsorbed\ oil\ (g)}{weight\ of\ sponge\ (g)} \quad (3)$$

3. Results and discussion

3.1. Characteristics of the soot

The thermal characteristics of the soot were quantified with TGA under both air and nitrogen atmospheres to determine the oxidation behavior and thermal stability, respectively (Fig. 4). As a function of temperature, the thermogravimetric weight loss curve (TG) and the weight loss derivative curve (dTG) were recorded and compared. During oxidation, the soot sample exhibited a single broad mass loss within the temperature range of 460–700 °C which is apparent on the dTG curve. This single-step oxidation reaction is similar to that of carbon black and graphite samples, whereas typically two-step oxidation was observed for diesel soot samples indicating the combustion of soluble and volatile organic fractions [31]. After about 700 °C, the dTG curve reached an asymptotic value and the remaining mass was 3.1 % of the initial sample mass at that temperature while it was 1.2 % at 1000 °C. In other words, complete oxidation of the carbonaceous soot was nearly accomplished at higher temperatures with a minor amount of residue. The thermogram of the soot sample heated under nitrogen atmosphere is also displayed in Fig. 4. As seen, the total mass loss was significantly low, approximately 7.7 %, and no notable mass loss rate was observed in the dTG curve. By comparison, the mass losses for air and nitrogen atmosphere thermograms were recorded as 98.8 and 7.7 %, respectively. Considering the thermal stability of carbonaceous materials under inert atmosphere, it could be admitted that the soot sample showed high stability against high temperatures, which could be advantageous during its utilization for separation processes.

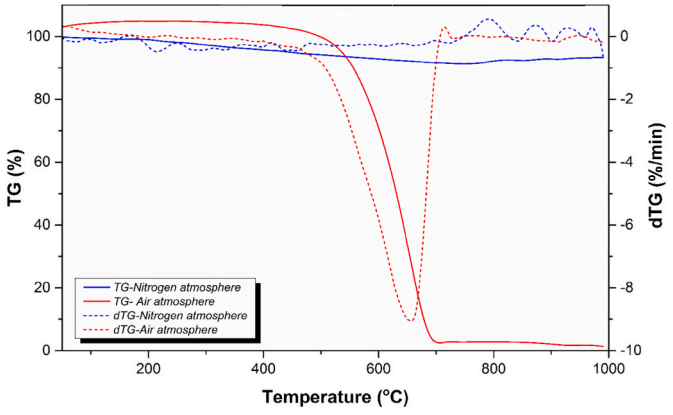

Fig. 4. Thermal stability (nitrogen atmosphere) and oxidation (air atmosphere) behavior of soot sample.

The particle size distribution of the soot sample by intensity, volume, and number percent is given in Fig. 5. According to Rayleigh's approximation, the intensity of scattering of a particle is proportional to the sixth power of its diameter [32] and hence DLS is an effective tool to understand the particle size distribution. The basic distribution obtained from DLS is the intensity data and the others are generated from this. The average particle size is recorded to be 835 nm and as can be seen from the number size distribution analysis the diameter of the particles is between 342 and 2000 nm with a major peak at approximately 531 nm. Repeated analyses showed consistent results among themselves which indicated soot particles retain their stability in size even after being subjected to sonification. There are not any observed particle growth and agglomeration which increases the mean particle size.

To observe the surface morphology of the particles together with chemical analysis, SEM-EDX spectra of the produced soot were captured (Fig. 6). Irregularly shaped compact aggregates with a structure including almost spherical soot particles are obviously seen in the micrographs. Furthermore, the irregular edges of the soot may indicate

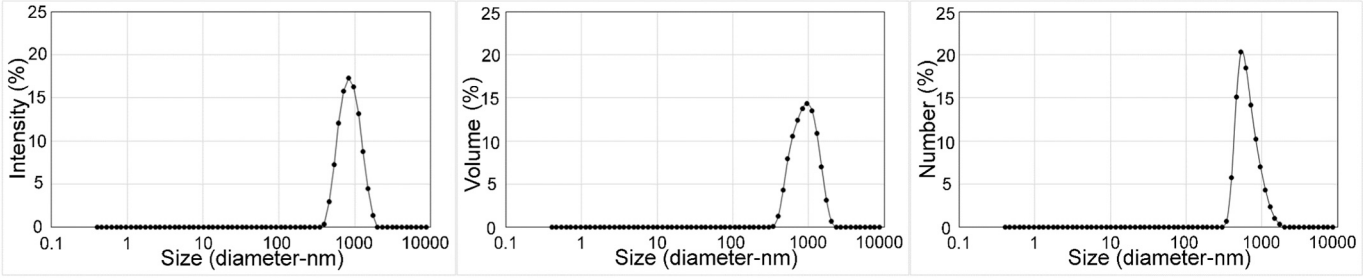

Fig. 5. Particle size distributions of the soot in intensity, volume, and number.

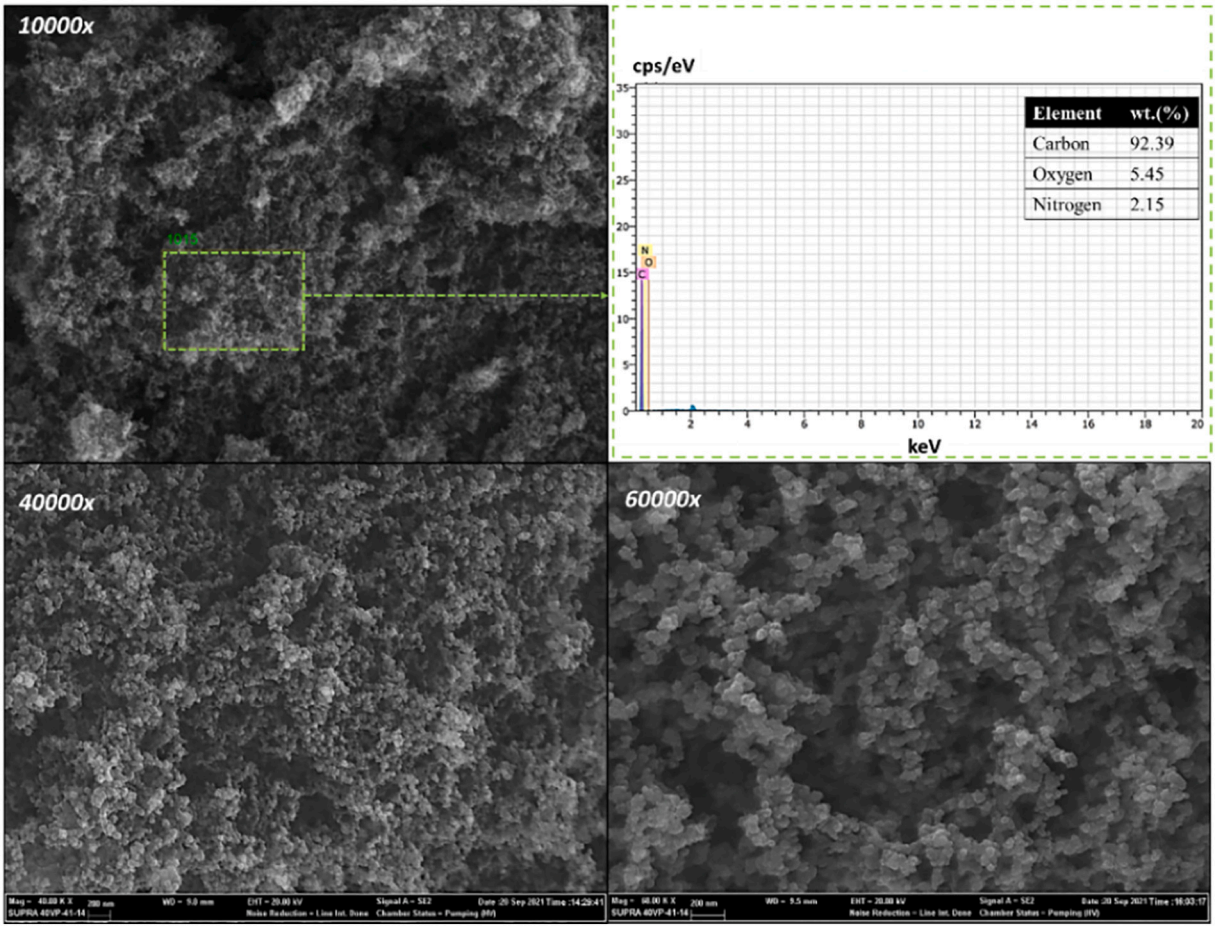

Fig. 6. SEM-EDX analysis of the soot sample at different magnifications.

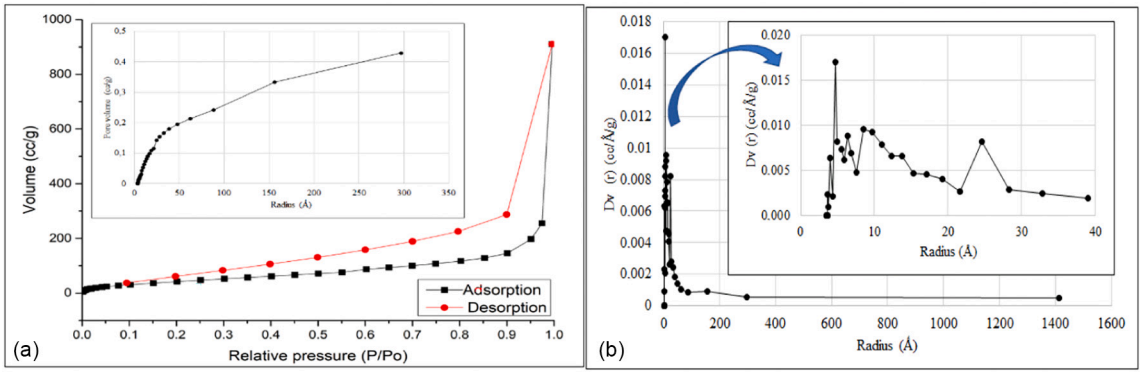

Fig. 7. (a) N_2 adsorption-desorption isotherm and (b) pore size distribution of soot sample.

defects in the carbonaceous network arising from the presence of sp^3 carbon [33]. The particles with a heterogeneous surface may enhance the oil removal process by creating sites to adhere to the surface. From SEM-EDX analysis, the carbon content of the soot is reported as >92 wt %. In addition, minor amounts of oxygen and nitrogen are situated in the structure but pure carbon without any contamination is present during synthesis.

To characterize the porous structure of the soot, N_2 adsorption and desorption isotherms were obtained in the range of 0.001 and 0.9961 P/P_o as given in Fig. 7.a. Brunauer–Emmett–Teller (BET) surface area [34] of the soot was quantitatively determined via selected points of the adsorption isotherm, while pore size distribution was estimated with Barrett−Joyner−Halenda (BJH) method [35].

The obtained isotherm exhibited a shape that is characterized by a mesoporous structure. The hysteresis loop, non-overlapping branches of adsorption, and desorption branches of isotherm, in Fig. 7.a, indicate a mesoporous character of the synthesized soot [36,37]. At the same time, a progressive increase in volume adsorbed in the entire range of P/P_o is an indicator of a mesoporous nature of the carbon [38]. The isotherm has a hysteresis loop and its exact shape varies from one adsorption system to another due to capillary condensation. According to the results, the total nitrogen adsorbed was 910.1 $cm^3 \cdot g^{-1}$ while BET surface area was calculated to be 175.7 $m^2 \cdot g^{-1}$. Accordingly, the total pore volume was estimated to be 1.411 $cm^3 \cdot g^{-1}$ at $P/P_o = 0.9961$. Fig. 7.b shows the pore size distribution of the soot sample representing that the diameter of the majority of the pores lies in the range of 6–320 Å with a peak value of about 10 Å. In addition to the N_2 adsorption-desorption analysis, the real density of the soot was determined as 1.7783 ± 0.0005 $g \cdot cm^{-3}$ using the He pycnometer.

The functional group analysis of the soot sample was performed with an FT-IR spectrometer and the spectrum is given in Fig. 8.a. Weak peaks of symmetric and asymmetric stretching vibrations attributed to the presence of CH_2 and CH_3 groups are observed for the sample between 2950 and 2860 cm^{-1}. The band between 1566 and 1650 cm^{-1} is assigned to the presence of C═C stretching vibrations arising from the alkene structure. The characteristic strong peaks for C—O stretching vibrations appear between 1275 and 1200 cm^{-1} and 1075–1020 cm^{-1} revealing the fact that during the formation of soot minor amounts of oxygenated compounds also formed [39]. Moreover, the plain spectrum showed that the soot sample does not contain overly complicated functional groups and the material is composed of amorphous carbon having sp^2 and sp^3 configurations. As a result of the Raman spectroscopy study of the sample (Fig. 8.b), the two characteristic bands (G and D bands) for amorphous carbon are observed. The spectrum exhibits a strong peak (G band) with a maximum intensity at around 1570 cm^{-1} that can be assigned to the ideal graphitic lattice vibrations. The second broadband (D band), which is noticed at around 1350 cm^{-1}, is due to the disordered graphitic lattice. The D-peak is associated with defects in the sample structure, whereas the G band refers to tangential C—C valence oscillations. The G-band is sensitive to stress in the sample structure. The third significant broadband in the range of about 2500 cm^{-1} to 3250 cm^{-1} is observed from the spectrum, which can be attributed to the overlapping of second-order bands resulting from the graphitic lattice vibration modes [40].

The graphitic character of the soot sample was further investigated via XRD and PDXL software was used for the analysis of the profile (Fig. 8.c). The two main Bragg diffraction peaks are observed. The XRD peak around $2\theta \approx 26.23^\circ$, indexed as C (002), represents the amorphous structure of carbon materials, and the second peak around $2\theta \approx 42.21^\circ$, indexed as (100) plane is an indication of the low crystalline structure (ICDD card # 1200017). The interlayer spacing (d_{002}) equal to 0.3611 nm, which is in the typical ranges (0.3591–0.3679 nm) of soot samples prepared from different gases under different conditions, was calculated using Eq. (2) [41–43]. The interlaying spacing of the soot sample is larger than the non-graphitized crystal interlaying spacing, and thus the graphitization degree is calculated to be −198.8 %. It is obvious that the amorphous structured soot sample showed a significantly low degree of graphitization.

3.2. Characteristics of soot-coated hydrophobic sponge

Raw melamine sponge was used as the substrate material for soot particles. Foam like structured hydrophilic melamine sponge was coated with carbon soot to achieve a hydrophobic surface for its further utilization in oil-water separation processes. The attachment and well-distribution of soot particles on the surface is an important phenomenon and can be carried out simply via the dip and dry method. During the interaction of sponge and soot particles, the three-dimensional (3D) structure of pristine melamine sponge with its interconnected network and high porosity of over 99 % ensured the proper distribution of soot and prevented the agglomeration of the particles [25,44]. It is evident from the photograph of the sponge that the melamine sponge, initially white, was completely covered with soot (the final color is black) after a successive dip and dry process (Fig. 9). The surface morphology of the raw and soot-coated sponge samples was carried out by SEM and the images are also presented in Fig. 9. As described in previous papers [20,45], SEM micrographs demonstrate the three-dimensional hierarchical porous structure of the sponge. The micrograph of the sorbent shows the available adsorption sites which may be accessible by the sorbate molecules [46]. Soot is strongly attached to the skeleton of the melamine sponge due to the van der Waals interactions between the soot and the sponge. The nanoscale porous surface and the hierarchical porous structure contribute to the hydrophobicity of the superhydrophobic sponge and thus provide high efficiency in adsorbing oil. It is well known that sorbents need to have the ability to hold the sorbate oils in their voids once they are sucked up to maintain a better oil-water separation. Therefore, a hydrophobic, preferably superhydrophobic, and oleophilic surface is required to enhance the capacity and recyclability of the sorbent [47]. Compared with the raw sponge, the SEM image shows the soot-coated sponge retained the microporous structured-3D framework. Although a noticeable thickening was observed in the framework struts after the soot coating, a uniform distribution of soot was clearly monitored since there was no agglomeration on the edges or the struts. The image obtained at higher

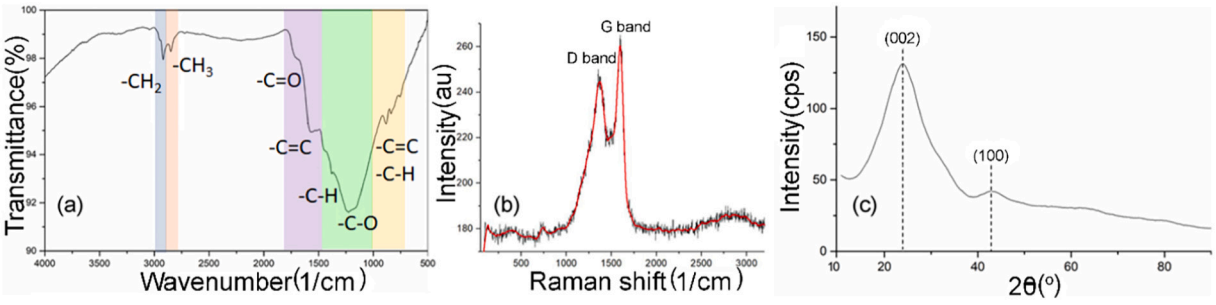

Fig. 8. (a) FT-IR spectrum, (b) Raman spectrum, and (c) XRD profile of soot sample.

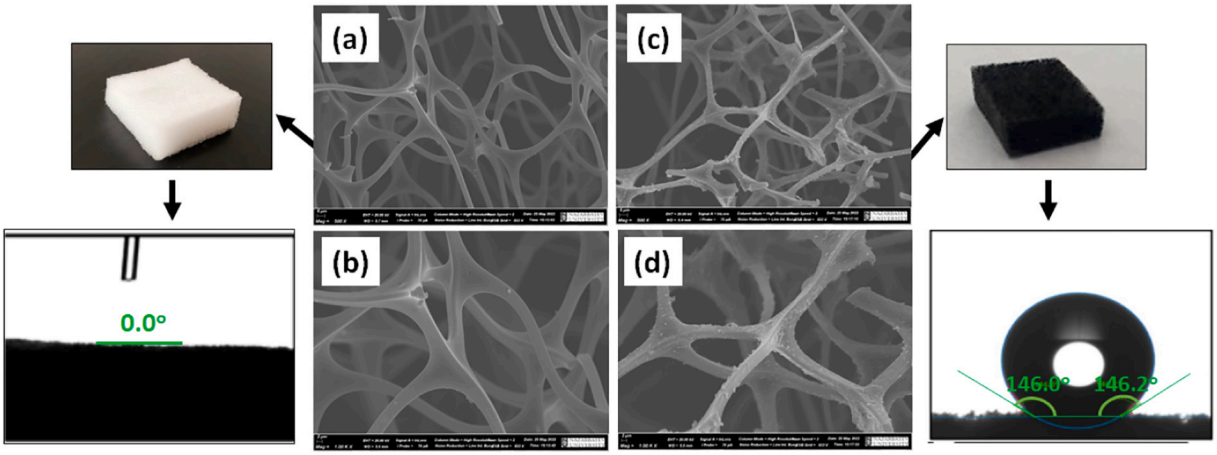

Fig. 9. The water contact angle and SEM images of the melamine sponge before (a, b) and after the soot coating process (c, d).

magnifications also revealed the fact that soot nanoparticles were successfully attached to the framework struts.

The hydrophobicity of the surface of soot coated sponge was evaluated using the contact angle test results. The water contact angle of the sponge surface was ~145–150°, indicating superior hydrophobicity (Fig. 9). This is due to the high hydrophobicity of the soot prepared from the propane-butane mixture. On the other hand, the raw melamine sponge was completely hydrophilic as given in Fig. 3. It adsorbed water in its pores and sank to the bottom immediately. Similar work was reported by Gao et al. [20], where the soot was prepared from ethylene combustion and the water contact angle of the soot-coated sponge was determined between 140 and 145°.

3.3. Oil adsorption performance of hydrophobic sponge

The utilization of soot-coated sponges in the adsorption processes was investigated through their oil adsorption performance. For this purpose, the raw melamine sponge, after being washed (with acetone) and dried, was used to remove oil residues from the water surface. It was observed that the pure melamine sponge adsorbs oil. Since the sponge showed hydrophilic properties, it simultaneously adsorbed water and was immersed in it, not completely adsorbing the oil from the surface. On the other hand, as shown by the melamine sponge coated with soot in Fig. 3, the high contact angle (hydrophobic character) and low density made it float easily on the water surface and completely adsorbed oil residue from the surface. The mass of oil adsorbed by the sponge was found by the difference between the mass of the sponge after and before sorption. Once the sponge has been placed over the surface of the oil-water the floating sponge adsorbed the oil rapidly and completely. During the experiments, soot coated melamine sponge with a total surface area of 16 cm^2, a volume of 4 cm^3, and a mass of ~0.086 g was used to adsorb about 2.08 ± 0.50 g of petroleum oil which corresponds to an average adsorption capacity of 23.40 $g{\cdot}g^{-1}$ as shown in Fig. 10. The adsorption capacity of the soot-coated melamine sponge was found to be close to that of carbonized asphalt-melamine sponge which was used for the removal of several oil types such as diesel (33 $g{\cdot}g^{-1}$), soybean oil (37 $g{\cdot}g^{-1}$), and pumping oil (41 $g{\cdot}g^{-1}$) [45]. Another carbon-coated melamine sponge (modified with silk fibroin-graphene oxide) also exhibited a sorption capacity of ~55 $g{\cdot}g^{-1}$ for the separation of silicon oil from water [48]. Moreover, sorption capacities of 17–43 $g{\cdot}g^{-1}$ were reported for carbon-based magnetic superhydrophobic sponges for the adsorption of oils and organic solvents [49]. As can be recognized, compared to the previously reported oil adsorption capacities, the soot-coated melamine sponge showed an acceptable level of sorption capability.

The reusability of hydrophobic sponge materials is an important property for its utilization in the sorption processes [50]. In this study, the reusability of the soot-coated sponge was tested by simply squeezing the sponge and drying it. Due to its high hydrophobicity and porous structure, the prepared sponge allowed the oil to be squeezed out completely up to 19 times by cleaning the water surface (Fig. 10). After 20 times of use, the cleaning efficiency gradually decreased. During the experiments, this was also confirmed by the fact that an oily layer of yellow color remained on the surface of the water. The rectangular prism-shaped melamine sponge did not lose its shape during the absorption-desorption cycles up to 5 times. Although the sponge lost its original shape after the 5th trial, there was no decrease in its sorption ability and it cleaned the water surface properly. When the sorption cycles are compared to that of other sponge samples reported in the literature, it is seen that the soot-coated hydrophobic sponge achieved a high repeated usage [50,51]. In addition, the average oil removal speed of the soot-coated melamine sponge was determined to be 1.14 ± 0.1 s as an average value of 25 adsorption cycles.

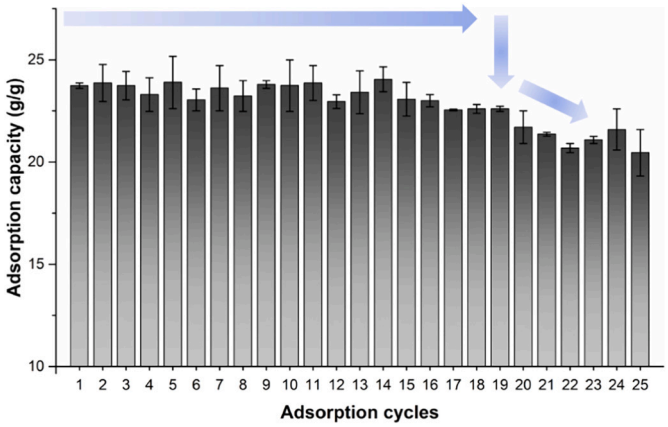

Fig. 10. Repeatability of sorption properties of hydrophobic sponge.

During the adsorption of petroleum oil on the soot-coated melamine sponge, multiple adsorption mechanisms may act together [52]. Since the sizes of the superhydrophobic carbonaceous soot are so small, which creates a porous structure, a probable combined mechanism of adsorption may be included. These mechanisms are hydrophobic interaction, capillary effect into interparticle/intraparticle soot particles together with physical non-covalent interactions such as Van der Waals forces and hydrogen bonding. The presence of a hydrophobic structure with sp^2 hybridized carbon may also present the possibility of π-π bonding with the aromatic rings [53] of petroleum oil. Some fluctuations

between the cycles may be attributed to the interlace effect, in which the sponge acts as a network, getting around the drops of petroleum oil and trapping them. Moreover, accessible sorption sites may be blocked between cycles may cause a slight decline in the sorptive capacity of the sponge.

To test the acid and alkali resistance of the produced sponge, HCl and NaOH-treated samples were subjected to various mechanical deformations including compressing, bending and twisting. As can be seen from Fig. 11, the sponges retained their original forms without any visible plastic deformation, suggesting their good elasticity and recyclability. Furthermore, the soot-coated sponges captured dynamic water droplet shedding and retained their spherical shape after acid and alkali treatment. The resultant soot-coated sponge was also reasonable enough in acid and alkaline environments attributing to its stable carbonaceous networks. The soot-coated sponge had outstanding mechanical and hydrophobic stability in acidic and basic conditions, which are crucial for feasible oil-water separation applications that may include pH variations during the operation. Therefore, it may hold a promising application for long-term oil separation processes unless it is not subjected to higher loadings. On the other hand, mechanical test results showed that acidic and basic conditions behaved differently. The tensile strength and elongation at break values were calculated for pristine melamine sponge as 0.04 MPa and 43.9 % respectively, while soot-coated sponge yielded tensile strength of 0.07 MPa and elongation of 45.4 %. The results showed that the mechanical strength of the soot-coated sponge was slightly higher than that of the melamine sponge. When the product had been subjected to the acidic treatment, its tensile strength decreased remarkably to 0.01 MPa, and elongation at break was calculated as 38.8 %. On the other hand, the tensile strength of the alkali-treated soot-coated sponge was found nearly the same compared to the product without any chemical treatment while the elongation value had increased up to 60 %. As a result, the alkaline-treated and coated sponge had shown the highest elongation among the pristine, soot-coated, and acid-treated melamine sponges. The pH of the water or any pretreatment applied to the sponge prior to its usage affects the lifetime of the sorbent material which can be settled by a sensitive adjustment of the operating conditions of the sorption. And hence the efficiency of the sorption process and as well as the stability of the sorbent material can be preserved even under mild changes in the process conditions.

The relevant studies on the oil removal processes by adsorption and their main findings are summarized in Table 1. The researchers have focused on finding an effective sorbent with high oil sorption and low water uptake. Some studies investigated natural materials such as biomass and its modified forms while others aimed to synthesize sorbents using inorganic channeled structures such as zeolites. As can be understood from the table, the produced sponge is perceived to be attractive for the removal of petroleum oil spills among the sorbents identified in the literature for water treatment. Undoubtedly, the reusability of a sorbent is one of the critical parameters in determining its effectiveness for wastewater treatment [54]. As it can be seen, the sorptive structure of the sponge obtained in this work is compatible with the sorbents that were produced with different precursors and production methods. Most importantly the reusability is found to be the highest among the studies including the removal of petroleum oil and its derivatives from water.

4. Conclusions

This current study shows the effect of soot coating on a melamine sponge, pointing to a useful technique for the production of highly effective materials for practical oil contaminant cleanup via adsorption processes. The soot with a hydrophobic character was synthesized from a propane-butane gas mixture and then a melamine sponge was coated with soot using the facile dip and dry method. In this respect, simple and cost-effective procedures were used to prepare selective sorbent for petroleum oil. The adsorption-desorption cycles demonstrated that the sponge is highly efficient and stable. The selectivity of soot-coated melamine sponge towards oil was found to be excellent with a capacity of up to ~24 times its weight, along with recyclability of >19 times. Based on the characteristics, soot-coated sponges could be recycled and reused many times with considerable capacity retention towards petroleum oil. Moreover, the sorption sites of the carbon material coated sponge were not destroyed by the acid and alkali environment and hydrophobicity retention with acceptable minor changes in the mechanical properties (tensile strength) of the sponge was maintained after these corrosive procedures. As a result, this material emerges as a promising high-quality sorbent for the separation of petroleum oil from water, and it can be advantageous in wastewater recovery in the industry. An in-

Fig. 11. Mechanical stabilities of (a) coated sponge, (b) after acid, and (c) alkali treatment.

Table 1
Comparison of sorption capacities of various natural and synthetic sorbents for the removal of petroleum and its derivatives.

Sorbent	Sorbate	Maximum sorption capacity ($g \cdot g^{-1}$)	Number of reuses	Reference
Nettle fibers	Crude oil	8.32	N/A	[55]
Acetylated nettle fibers		18.75		
Orange peels (OPs)	Crude oil	5.00	5	[56]
Thermally modified OPs		~7.25	N/A	
Palm fibers	Diesel oil	35.71	N/A	[57]
	Crude oil	22.73		
Pineapple leaves (PLs)	Crude oil	~0.04	N/A	[58]
Lauric acid-modified PLs		~0.11		
Stearic acids modified PLs		~0.14		
Pistia leaves	Crude oil	~2.90	N/A	[59]
Pistia roots		~2.32		
Pomelo peel (PP)	Diesel oil	6.39	N/A	[60]
	Lubricating oil	9.04		
Anhydride-treated PP	Diesel oil	16.50		
	Lubricating oil	19.39		
Styrene-treated PP	Diesel oil	18.91		
	Lubricating oil	26.36		
Thermally treated rice husks	Crude oil	15.00	N/A	[61]
Wheat straw	Diesel oil	~24.21	N/A	[62]
Sugarcane bagasse	Gasoline	12.00	N/A	[63]
Sugarcane bagasse (SB)	Crude oil	6.00	N/A	[64]
Acetylated SB		11.30		
Gelatin/gum Arabic hybrid hydrogels	Crude oil	1.53	N/A	[65]
Fatty acid-modified pinewood biochar	Crude oil	5.32	>5	[66]
Polydimethylsiloxane–graphene sponge	Gasoline	6.50	N/A	[67]
Carbon/fly ash composite	Petroleum oil	1.39	N/A	[68]
Zeolite/carbon composites (from faujasite)		1.54		
Zeolite-carbon composite (from gismondite)		1.69		
C/SiO_2 composite (from carbonized rice husk)	Gasoline	3.70	N/A	[69]
	Diesel oil	5.50		
	Light crude oil	6.00		
Cellulose aerogels	Petroleum oil	~23.19	N/A	[69]
Chitin flakes	Crude oil	~0.26	N/A	[70]
Chitin powder		~0.17		
Chitosan flakes		~0.38		
Chitosan powder		~0.28		
Chitosan solution		~0.01		
Hydrophobic soot-coated melamine sponge	Crude oil	24.00	19	This study

depth assessment of factors affecting adsorption with optimization studies offers the potential to boost the capacity of the as-prepared sponge even further.

Declaration of competing interest

The authors declare that they have no known competing financial interests or personal relationships that could have appeared to influence the work reported in this paper.

Data availability

Data will be made available on request.

Acknowledgments

This research has been funded by the Science Committee of the Ministry of Education and Science of the Republic of Kazakhstan (Grant No. AP08856321). The authors also acknowledge Malika Tulegenova for her technical assistance in the laboratory.

References

[1] M. Anjum, R. Miandad, M. Waqas, F. Gehany, M. Barakat, Remediation of wastewater using various nano-materials, Arab. J. Chem. 12 (8) (2019) 4897–4919.
[2] R. Molinari, L. Palmisano, E. Drioli, M. Schiavello, Studies on various reactor configurations for coupling photocatalysis and membrane processes in water purification, J. Membr. Sci. 206 (1–2) (2002) 399–415.
[3] S. Bandehali, F. Parvizian, H. Ruan, A. Moghadassi, J. Shen, A. Figoli, A.S. Adeleye, N. Hilal, T. Matsuura, E. Drioli, A planned review on designing of high-performance nanocomposite nanofiltration membranes for pollutants removal from water, J. Ind. Eng. Chem. 101 (2021) 78–125.
[4] D. Kapoor, M.P. Singh, Heavy metal contamination in water and its possible sources, in: HeavyMetals in the Environment, Elsevier, 2021, pp. 179–189.
[5] C. Guigue, L. Bigot, J. Turquet, M. Tedetti, N. Ferretto, M. Goutx, P. Cuet, Hydrocarbons in a coral reef ecosystem subjected to anthropogenic pressures (La Réunion Island, Indian Ocean), Environ. Chem. 12 (3) (2015) 350–365.
[6] J. Sayyad Amin, M. Vared Abkenar, S. Zendehboudi, Natural sorbent for oil spill cleanup from water surface: environmental implication, Ind. Eng. Chem. Res. 54 (43) (2015) 10615–10621.
[7] Y. Liang, D. Wang, H. Chen, Preparation of high oil absorption resins by suspended emulsion polymerization and their properties, Sep. Sci. Technol. 48 (13) (2013) 1977–1981.
[8] L. Mohammadi, A. Rahdar, E. Bazrafshan, H. Dahmardeh, M. Susan, A.B. Hasan, G. Z. Kyzas, Petroleum hydrocarbon removal from wastewaters: a review, Processes 8 (4) (2020) 447.
[9] J.C. Onwuka, E.B. Agbaji, V.O. Ajibola, F.G. Okibe, Treatment of crude oil-contaminated water with chemically modified natural fiber, Appl. Water Sci. 8 (3) (2018) 1–10.
[10] Y. Yihdego, R.A. Al-Weshah, Engineering and environmental remediation scenarios due to leakage from the Gulf war oil spill using 3-D numerical contaminant modellings, Appl Water Sci 7 (7) (2017) 3707–3718.
[11] T. Zhang, Z. Li, Y. Lü, Y. Liu, D. Yang, Q. Li, F. Qiu, Recent progress and future prospects of oil-absorbing materials, Chin. J. Chem. Eng. 27 (6) (2019) 1282–1295.
[12] F.I. Alghunaimi, D.J. Alsaeed, A.M. Harith, T.A. Saleh, Synthesis of 9-octadecenoic acid grafted graphene modified with polystyrene for efficient light oil removal from water, J. Clean. Prod. 233 (2019) 946–953.
[13] C.H. Lee, B. Tiwari, D. Zhang, Y.K. Yap, Water purification: oil–water separation by nanotechnology and environmental concerns, Environ. Sci. Nano 4 (3) (2017) 514–525.
[14] M. Mojžiš, T. Bubeníková, M. Zachar, D. Kačíková, J. Štefková, Comparison of natural and synthetic sorbents' efficiency at oil spill removal, Bioresources 14 (4) (2019) 8738–8752.
[15] S. Gupta, N.-H. Tai, Carbon materials as oil sorbents: a review on the synthesis and performance, J. Mater. Chem. A 4 (5) (2016) 1550–1565.
[16] N. Ohta, Y. Nishi, T. Morishita, Y. Ieko, A. Ito, M. Inagaki, Preparation of microporous carbon foams for adsorption/desorption of water vapor in ambient air, New Carbon Mater. 23 (3) (2008) 216–220.

[17] X.-Q. Zhang, W.-C. Li, A.-H. Lu, Designed porous carbon materials for efficient CO2 adsorption and separation, New Carbon Mater. 30 (6) (2015) 481–501.
[18] F.A. Abu Al-Rub, J. Hamdi, N. Hamdi, H. Allaboun, M. Al Zarooni, M. Al-Sharyani, Adsorption of phenol on different activated carbons prepared from date pits, Sep. Sci. Technol. 46 (2) (2010) 300–308.
[19] Y. Zhang, L. Qin, Y. Cui, W.-F. Liu, X.-G. Liu, Y.-Z. Yang, A hydrophilic surface molecularly imprinted polymer on a spherical porous carbon support for selective phenol removal from coking wastewater, New Carbon Mater. 35 (3) (2020) 220–231.
[20] Y. Gao, Y.S. Zhou, W. Xiong, M. Wang, L. Fan, H. Rabiee-Golgir, L. Jiang, W. Hou, X. Huang, L. Jiang, Highly efficient and recyclable carbon soot sponge for oil cleanup, ACS Appl. Mater. Interfaces 6 (8) (2014) 5924–5929.
[21] P. Li, Q. Cai, W. Lin, B. Chen, B. Zhang, Offshore oil spill response practices and emerging challenges, Mar. Pollut. Bull. 110 (1) (2016) 6–27.
[22] F. Beshkar, H. Khojasteh, M. Salavati-Niasari, Recyclable magnetic superhydrophobic straw soot sponge for highly efficient oil/water separation, J. Colloid Interface Sci. 497 (2017) 57–65.
[23] M. Nazhipkyzy, A. Nurgain, M. Florent, A. Policicchio, T.J. Bandosz, Magnetic soot: surface properties and application to remove oil contamination from water, J. Environ. Chem. Eng. 7 (3) (2019), 103074.
[24] S. Liu, Q. Xu, S.S. Latthe, A.B. Gurav, R. Xing, Superhydrophobic/superoleophilic magnetic polyurethane sponge for oil/water separation, RSC Adv. 5 (84) (2015) 68293–68298.
[25] Y. Feng, J. Yao, Design of melamine sponge-based three-dimensional porous materials toward applications, Ind. Eng. Chem. Res. 57 (22) (2018) 7322–7330.
[26] J. Zhao, Q. Guo, X. Wang, H. Xie, Y. Chen, Recycle and reusable melamine sponge coated by graphene for highly efficient oil-absorption, Colloids Surf. A Physicochem. Eng. Asp. 488 (2016) 93–99.
[27] L. Zhang, L. Feng, X. Gu, C. Zhang, Superelastic and hydrophobic-oleophilic modified melamine foam by ultralow amount of graphene for oil/water separation, J. Appl. Polym. Sci. 138 (11) (2021) 50038.
[28] L. Zou, B. Huang, Y. Huang, Q. Huang, C.A. Wang, An investigation of heterogeneity of the degree of graphitization in carbon–carbon composites, Materials Chemistry and Physics 82 (3) (2003) 654–662, https://doi.org/10.1016/S0254-0584(03)00332-8.
[29] A. Vlahov, XRDGraphitization Degrees: A Review of the Published Data and New Calculations,Correlations, and Applications, 2021.
[30] B. Jiang, P. Wang, Y. Ying, M. Luo, D. Liu, Nanoscale characteristics and reactivity of nascent soot from n-heptane/2, 5-dimethylfuran inverse diffusion flames with/without magnetic fields, Energies 11 (7) (2018) 1698.
[31] S. Eichholz, M. Lerch, M. Heck, D. Walter, Various carbon dust particles: studies on thermal behaviour, J. Therm. Anal. Calorim. 110 (1) (2012) 437–441.
[32] J. Stetefeld, S.A. McKenna, T.R. Patel, Dynamic light scattering: a practical guide and applications in biomedical sciences, Biophys. Rev. 8 (4) (2016) 409–427.
[33] V. Gargiulo, M. Alfè, G. Di Blasio, C. Beatrice, Chemico-physical features of soot emitted from a dual-fuel ethanol–diesel system, Fuel 150 (2015) 154–161.
[34] S. Brunauer, P.H. Emmett, E. Teller, Adsorption of gases in multimolecular layers, J. Am. Chem. Soc. 60 (2) (1938) 309–319.
[35] E.P. Barrett, L.G. Joyner, P.P. Halenda, The determination of pore volume and area distributions in porous substances. I. Computations from nitrogen isotherms, J. Am. Chem. Soc. 73 (1) (1951) 373–380.
[36] S. Lowell, J.E. Shields, M.A. Thomas, M. Thommes, Characterization of Porous Solids and Powders: Surface Area, Pore Size and Density, Springer Science & Business Media, 2006.
[37] M. Muttakin, S. Mitra, K. Thu, K. Ito, B.B. Saha, Theoretical framework to evaluate minimum desorption temperature for IUPAC classified adsorption isotherms, Int. J. Heat Mass Transf. 122 (2018) 795–805.
[38] K.S.K. Reddy, A. Al Shoaibi, C. Srinivasakannan, A comparison of microstructure and adsorption characteristics of activated carbons by CO2 and H3PO4 activation from date palm pits, New Carbon Mater. 27 (5) (2012) 344–351.
[39] V. Ţucureanu, A. Matei, A.M. Avram, FTIR spectroscopy for carbon family study, Crit. Rev. Anal. Chem. 46 (6) (2016) 502–520.
[40] A. Sadezky, H. Muckenhuber, H. Grothe, R. Niessner, U. Pöschl, Raman microspectroscopy of soot and related carbonaceous materials: spectral analysis and structural information, Carbon 43 (8) (2005) 1731–1742.
[41] Y. Ying, C. Xu, D. Liu, B. Jiang, P. Wang, W. Wang, Nanostructure and oxidation reactivity of nascent soot particles in ethylene/pentanol flames, Energies 10 (1) (2017), https://doi.org/10.3390/en10010122.
[42] Y. Liu, C. Song, G. Lv, C. Fan, X. Zhang, Y. Qiao, Relationships between the electrical properties and nanostructure of soot particles in a laminar inverse diffusion flame, Proc. Combust. Inst. 37 (1) (2019) 1185–1192, https://doi.org/10.1016/j.proci.2018.06.090.
[43] B. Jiang, P. Wang, Y. Ying, M. Luo, D. Liu, Nanoscale characteristics and reactivity of nascent soot from n-heptane/2,5-dimethylfuran inverse diffusion flames with/without magnetic fields, Energies 11 (7) (2018), https://doi.org/10.3390/en11071698.
[44] P. Hong, Z. Liu, Y. Gao, Y. Chen, M. Zhuang, L. Chen, X. Liu, H. Xiang, Fabricated of superhydrophobic silanized melamine sponge with photochromic properties for efficiency oil/water separation, Adv. Polym. Technol. 2019 (2019).
[45] Q. Yao, P. Zhao, R. Li, C. Li, Y. Luo, G. Zhou, M. Yang, Fabrication of recyclable carbonized asphalt-melamine sponges with high oil-absorption capability, J. Chem. Technol. Biotechnol. 92 (6) (2017) 1415–1420.
[46] T.A. Saleh, Isotherm, kinetic, and thermodynamic studies on Hg (II) adsorption from aqueous solution by silica-multiwall carbon nanotubes, Environ. Sci. Pollut. Res. 22 (21) (2015) 16721–16731.
[47] Z. Wang, H. Ma, B. Chu, B.S. Hsiao, Super-hydrophobic polyurethane sponges for oil absorption, Sep. Sci. Technol. 52 (2) (2017) 221–227.
[48] J. Zhou, Y. Zhang, Y. Yang, Z. Chen, G. Jia, L. Zhang, Silk fibroin-graphene oxide functionalized melamine sponge for efficient oil absorption and oil/water separation, Appl. Surf. Sci. 497 (2019), 143762.
[49] N. Wang, Z. Deng, Synthesis of magnetic, durable and superhydrophobic carbon sponges for oil/water separation, Mater. Res. Bull. 115 (2019) 19–26.
[50] G.B. Demirel, E. Aygül, Robust and flexible superhydrophobic/superoleophilic melamine sponges for oil-water separation, Colloids Surf. A Physicochem. Eng. Asp. 577 (2019) 613–621.
[51] B. Li, X. Liu, X. Zhang, J. Zou, W. Chai, Y. Lou, Rapid adsorption for oil using superhydrophobic and superoleophilic polyurethane sponge, J. Chem. Technol. Biotechnol. 90 (11) (2015) 2106–2112, https://doi.org/10.1002/jctb.4646.
[52] R.I. Kosheleva, G.Z. Kyzas, N.C. Kokkinos, A.C. Mitropoulos, Low-cost activated carbon for petroleum products clean-up, Processes 10 (2) (2022) 314.
[53] S. Khan, A. Achazhiyath Edathil, F. Banat, Sustainable synthesis of graphene-based adsorbent using date syrup, Sci. Rep. 9 (1) (2019) 1–14.
[54] I. Shittu, A.A. Edathil, A. Alsaeedi, S. Al-Asheh, K. Polychronopoulou, F. Banat, Development of novel surfactant functionalized porous graphitic carbon as an efficient adsorbent for the removal of methylene blue dye from aqueous solutions, journal of water, Process. Eng. 28 (2019) 69–81.
[55] S. Viju, G. Thilagavathi, B. Vignesh, R. Brindha, Oil sorption behavior of acetylated nettle fiber, J. Text. Inst. 110 (10) (2019) 1415–1423.
[56] I.A. El Gheriany, F.A. El Saqa, A.A.E.R. Amer, M. Hussein, Oil spill sorption capacity of raw and thermally modified orange peel waste, Alex. Eng. J. 59 (2) (2020) 925–932.
[57] O. Abdelwahab, S.M. Nasr, W.M. Thabet, Palm fibers and modified palm fibers adsorbents for different oils, Alex. Eng. J. 56 (4) (2017) 749–755.
[58] S.C. Cheu, H. Kong, S.T. Song, N. Saman, K. Johari, H. Mat, High removal performance of dissolved oil from aqueous solution by sorption using fatty acid esterified pineapple leaves as novel sorbents, RSC Adv. 6 (17) (2016) 13710–13722.
[59] G. Sánchez-Galván, F.J. Mercado, E.J. Olguín, Leaves and roots of Pistia stratiotes as sorbent materials for the removal of crude oil from saline solutions, Water Air Soil Pollut. 224 (2) (2013) 1–12.
[60] W. Chai, X. Liu, J. Zou, X. Zhang, B. Li, T. Yin, Pomelo peel modified with acetic anhydride and styrene as new sorbents for removal of oil pollution, Carbohydr. Polym. 132 (2015) 245–251.
[61] K. Kenes, O. Yerdos, M. Zulkhair, D. Yerlan, Study on the effectiveness of thermally treated rice husks for petroleum adsorption, J. Non-Cryst. Solids 358 (22) (2012) 2964–2969.
[62] E.X. Lv, Wuyang; tang, mingxiao; pu, yuewu, preparation of an efficient oil-spill adsorbent based on wheat straw, Bioresources 12 (1) (2017) 296–315.
[63] R. Behnood, B. Anvaripour, N.Jaafarzade Haghighi Fard, M. Farasati, Petroleum hydrocarbons adsorption from aqueous solution by raw sugarcane bagasse, Int J Emerg Sci Eng 1 (6) (2013) 96–99.
[64] R. Behnood, B. Anvaripour, N. Jaafarzadeh, M. Farasati, Oil spill sorption using raw and acetylated sugarcane bagasse, J. Cent. South Univ. 23 (7) (2016) 1618–1625.
[65] N. Scheverín, A. Fossati, F. Horst, V. Lassalle, S. Jacobo, Magnetic hybrid gels for emulsified oil adsorption: an overview of their potential to solve environmental problems associated to petroleum spills, Environ. Sci. Pollut. Res. 27 (1) (2020) 861–872.
[66] R. Gurav, S.K. Bhatia, T.-R. Choi, Y.-K. Choi, H.J. Kim, H.-S. Song, S.L. Park, H. S. Lee, S.M. Lee, K.-Y. Choi, Y.-H. Yang, Adsorptive removal of crude petroleum oil from water using floating pinewood biochar decorated with coconut oil-derived fatty acids, Sci. Total Environ. 781 (2021), 146636, https://doi.org/10.1016/j.scitotenv.2021.146636.
[67] D.N. Tran, S. Kabiri, T.R. Sim, D. Losic, Selective adsorption of oil–water mixtures using polydimethylsiloxane (PDMS)–graphene sponges, Environ. Sci.: Water Res. Technol. 1 (3) (2015) 298–305.
[68] L. Bandura, R. Panek, J. Madej, W. Franus, Synthesis of zeolite-carbon composites using high-carbon fly ash and their adsorption abilities towards petroleum substances, Fuel 283 (2021), 119173, https://doi.org/10.1016/j.fuel.2020.119173.
[69] D. Angelova, I. Uzunov, S. Uzunova, A. Gigova, L. Minchev, Kinetics of oil and oil products adsorption by carbonized rice husks, Chem. Eng. J. 172 (1) (2011) 306–311, https://doi.org/10.1016/j.cej.2011.05.114.
[70] F.C.D.F. Barros, L.C.G. Vasconcellos, T.V. Carvalho, R.F.D. Nascimento, Removal of petroleum spill in water by chitin and chitosan, Orbital: The Electronic Journal of Chemistry 6 (1) (2014) 70–74.